Regulation of adventitial interstitial fluid circulation by heartbeat and respiration

Hongyi Li*[1, 2†], Bei Li[1†], Wenqi Luo[3†], Xi Qi[4], You Hao[5], Chaozhi Yang[6], Wenqing Li[1], Jiazheng Li[7], Zhen Hua[7], Tan Guo[8], Zhijian Zheng[9], Xiaoxia Wang[10], Xue Yu[11], Xiaoxi Lv[12], Dahai Huang[2], Jun Hu[13,14], Zongmin Li[6], Fang Wang[11], Hua Li*[5], Chao Ma*[15,16], Fusui Ji*[11]

1. Research Center for Interstitial Fluid Circulation, 2. Department of Geriatrics, 3. Department of Cardiac Surgery, 4. Peking University Fifth School of Clinical Medicine, 7. Department of Anesthesiology, 8. Department of Radiology, 9. Department of Acupuncture, 10. Department of Endocrinology, 11. Department of Cardiology, Beijing Hospital, National Center of Gerontology, Institute of Geriatric Medicine, Chinese Academy of Medical Sciences, Beijing 100730, P.R. China

5. Institute of Computing Technology, Chinese Academy of Sciences, Beijing 100190, P.R. China

6. School of Computer Science and Technology, China University of Petroleum (East China), Qingdao 266580, P.R. China

12 State Key Laboratory of Bioactive Substance and Function of Natural Medicines, Institute of Materia Medica; Chinese Academy of Medical Sciences & Peking Union Medical College, Beijing, 100050, P.R. China

13 Key Lab of Interfacial Physics and Technology, Shanghai Institute of Applied Physics, Chinese Academy of Sciences, Shanghai 201210, P.R. China

14 Shanghai Synchrotron Radiation Facility, Shanghai Advanced Research Institute, Chinese Academy of Sciences, Shanghai 201210, P.R. China

15 Institute of Basic Medical Sciences, Chinese Academy of Medical Sciences, Department of Human Anatomy, Histology and Embryology, School of Basic Medicine, Peking Union Medical College, Beijing 100005, P.R. China

16 Chinese Institute for Brain Research, Beijing 100005, P.R. China

[†] These authors contributed equally to this work.

*Corresponding authors：

Hongyi Li, leehongyi@bjhmoh.cn; telephone number: +86 13911968580; address: No.1 Dong dan Dahua Road, Beijing 100730, P.R. China.

Fusui Ji, jifusui0367@bjhmoh.cn; telephone number: +86 13701120939; address: No.1 Dong dan Dahua Road, Beijing 100730, P.R. China.

Chao Ma, machao@ibms.cams.cn; telephone number: +86 13621000540; address: No.5 Dong dansantiao, Dongcheng District, Beijing 100005, P.R. China.

Hua Li, lihua@ict.ac.cn; telephone number: +86 13301275037; address: No.6 Kexueyuan South Road Zhongguancun Haidian District, Beijing 100190, P.R. China

Abstract

A growing body of evidence suggest that the interstitial fluid (ISF) may flow over long distance in the body. In this study, we aim to clarify the potential pathways of adventitial ISF flow and its regulatory mechanisms in rats with improved imaging methods. Fluorescent stereomicroscopy showed that each dilation or contraction of the heart and lungs can generate a to-and-fro motion of the adventitial ISF along the femoral veins following adventitial administration of Fluorescein sodium. Speckle tracking velocimetry revealed a positive regulation of the adventitial ISF flow by the heart rate under physiological conditions. Moreover, the ISF flow rate increased when breath was holding, and a pulsed ISF flow occurred during heavy breathing. In addition, silver nitrate was administered by adventitial or intravenous injection and spectral micro-computed tomography was adopted to compare the pathways of ISF or blood circulation, respectively. Our results indicated that the heart and lungs work synergistically to regulate the adventitial ISF flowing centripetally to the epicardium and myocardium, then into the lungs via pulmonary arteries and return to the heart via pulmonary veins, forming an adventitial ISF circulation. The adventitial ISF circulatory pathway might be a potentially novel route for organ-targeted extravascular drug delivery.

Key words: adventitia; interstitial fluid; circulation; cardiovascular system; respiration.

Introduction

Since the discovery of blood circulation by *Willian Harvey* in 1628, the interstitial fluid (ISF) is believed to mainly stay in the interstitial space and can only diffuse locally for fluid exchanges between vessels and tissues as described by *Starling's hypothesis* in 1896 [1-4]. However, long-standing efforts have explored that ISF may also flow around the body like the blood circulation. In the past several decades, a growing body of evidences indicated that the ISF could flow over a relatively long distance in certain tissue or organs, such as the interstitial tissue channels between capillaries and initial lymphatic vessels [5,6], the perivascular spaces in the brain and several other organs [7-9], the interstitial compartment of tumors [10,11], etc. Recently, by adopting *in vivo* fluorescent microscopy and magnetic resonance imaging techniques, our research group have revealed that the ISF can flow in the perivascular and adventitial connective tissues (PACTs) along certain blood vessels in animal models and human subjects [12-15]. In rabbits, the fluorescent ISF in ankle dermis was found to flow in the PACT pathways along the lower extremity veins, inferior vena cava in the abdomen and thorax, and into the pericardial cavity [12]. The estimated velocity of the fluorescent spots in adventitial ISF

along the femoral veins in the rabbit was 3.6~15.6 mm/s [15]. The arterial adventitial ISF flow was demonstrated in the lower limbs of the rabbits, mice and humans [13]. In the pulmonary circulation of rabbits, the adventitial ISF was found to flow along the pulmonary vein from the lungs toward the heart [15,16]. In the human cadaver experiments, ISF in the thumb skin could be "pulled" via the intact PACT pathways along the major veins of arm into the atrial walls when the heart was repeatedly compressed by an automatic cardiac compressor [14].

Although the long-range adventitial ISF flow has been observed, whether the ISF can circulate around the body and the pathway of ISF circulation is still not clear. Moreover, little is known about the regulatory mechanisms underlying the ISF flow or circulation. Limited by *in vivo* MRI, CT and other current imaging technique, it was difficult to distinguish the adventitial ISF flow from the intravascular blood flow [12-15]. In this study, using improved tracer imaging and quantitative speckle tracking techniques, we explored the potential pathways of adventitial ISF circulation and its regulatory mechanisms by heartbeat and respiration in the rat.

Results

Quantifying the longitudinal adventitial ISF flow along femoral artery and vein

Using fluorescent stereomicroscopy (Axio Zoom.V16, Zeiss) and the spectral micro-computed tomography (SMCT) [17-19], we examined which tracers were able to flow in the PACT pathways along the vessels of the lower limbs in rats, including several large (>1 kDa) and small (<1 kDa) molecular weight, water- and lipid-soluble tracers (Table S1). It was found that the fluorescein sodium (FluoNa) can be used for *in vivo* real-time fluorescent imaging, and the silver nitrate can be used for *in situ* imaging within tissues and organs (Figs. S1, Video 1). When the FluoNa was administrated to the PACT pathways on the saphenous vessels of rats, it could only be qualitatively observed that the fluorescein stained adventitial ISF flowed continuously along the femoral arteries and veins, inferior vena cava and into the cardiac surface (Figs. S1, S5). To quantitatively analyze the continuous flow of adventitial ISF, we experientially chose to observe the ISF flow in the PACT pathways along the femoral arteries and veins. When surgically opening the skin in the thigh to expose the femoral vessels, the fluorescent adventitial ISF flowing longitudinally along the femoral vessels and diffusing into the perivascular connective tissues can be readily recorded under the fluorescence stereomicroscopy.

After carefully removal of the perivascular connective tissues, a longitudinal adventitial ISF flow along the isolated femoral vein and artery could be clearly visualized after infusing the FluoNa (4 uL,

0.1 g/L, see Methods for detail) into the upstream PACT pathways on the saphenous vessels. At 30sec after the adventitial infusion, two linear fluorescent channels appeared on one side of the femoral vein, which was named as adventitial channel (Figs. 1b, 1b1, S2b). At 150 sec after the administration, the two adventitial channels were found to fuse into one adventitial channel (Figs. 1c, 1c1). Under real-time stereomicroscopy with a high-resolution camera (Prime BSI Scientific CMOS, Teledyne), a constant FluoNa flow can be clearly imaged in the linear adventitial channels along the femoral veins. The recorded FluoNa motions exhibited speckle-like between consecutive frames and matched closely the adventitial ISF flow along the vessels (Video 2). Limited by the current *in vivo* imaging technique, only the longitudinal flow of fluorescent ISF in the femoral arterial adventitia can be observed, but the speckle-like flow cannot be detected (Figs. 1c, 1c1).

If the adventitia along the femoral vein and artery were disrupted by type I collagenase, it was found that the upstream FluoNa cannot flow through and stain these femoral adventitial channels as well as the arterial wall (Figs. 1d, 1d1, S2c). At the same time, the angiography confirmed that both the femoral artery and vein were unobstructed (Fig. 1e, Videos 3, 4). Histological analysis of successive sections showed that the femoral artery and vein did not contain the vasa vasorum running continuously along the long axis of the vessels (Figs. S3a-j). The lymphatic vessels were also present in the perivascular connective tissues but not within the adventitia of blood vessels (Figs. S3k, S3l). Thus, the tunica adventitia surrounded by fascia, rather than a vascular conduit, were the histological structures for the longitudinal adventitial ISF flow.

To calculate the adventitial ISF flow rate along the vessels, we found that only the FluoNa can show the speckle-like flow of adventitial channels, while other Rhodamine B and Indocyanine green cannot. Accordingly, a speckle tracking velocimetry (STV) was performed (Fig. 1g) [20-23], and one of infusion doses, 4μl, was selected in the studies (Table S2). The amount of infusion fluid could not affect the velocity of adventitial ISF flow. In the 10-minute observation, we typically tracked around 130,000 speckles (Table S3). Under physiological conditions with the heart rate (HR) of 300-450 beats per minute (bpm) under anesthesia (respiratory rate of 60-90/min), the median velocity of the calculated speckles was around 588.2μm/sec (range 258.0 to 967.1μm/sec), and the mean velocity was 598.1±107.7μm/sec (Table S3). The velocity profiles showed that from the left edge of the linear adventitial channel, the ISF flow rate was uniform but not a parabola (Figs. 1h-k) [8,24,25]. By comparison, the calculated velocity of the arterial blood flow was 188.5±57.6mm/sec, and the venous blood flow 6.6±0.6mm/sec (Table S4).

Regulation of adventitial ISF flow along femoral vein by HR and respiration.

To identify the mechanisms of driving adventitial ISF flow under physiological conditions, we performed the STV to measure the adventitial ISF flow along the femoral veins (Fig.2a) while recording synchronized measurements of the electrocardiogram (ECG) and the respiratory cycle. Under physiological conditions, the flow rate of the adventitial ISF was associated with the HR and respiration. When the HR was reduced by the intravenous Esmolol, the flow rate of the adventitial ISF was decreased significantly (Figs. 2b). When the apnea was present and the HR was 410-420 bpm, the median flow rate of the adventitial ISF was significantly faster than that of resting breathing (Figs. 2c, 2c1). When breathing heavily with large amount of tidal volume, a pulsatile flow of the adventitial ISF was displayed, the frequency of which was the same as the heavy breath (Figs. 2c, 2c1).

Accordingly, we investigated the effects of the different respiratory parameters on the adventitial ISF flow in live or freshly deceased rats, respectively. When the HR was 390-420bpm, the frequency of the pulsed flow of the adventitial ISF was consistent with the respiratory rate (Figs. 2d, 2d1); at different tidal volumes, the greater the tidal volume is, the greater the pulse amplitude of the adventitial ISF flow (Figs. 2f, 2f1) is; the inspiration and expiration (I/E) ratio (1:1, 2:1, 1:2) determined the descending and ascending branches of the pulse (Figs. 2h, 2h1).

When the heart stopped beating and the lungs were ventilated repeatedly, the act of inhalation can cause a centrifugal flow of the adventitial ISF, while the act of exhalation induced a centripetal flow of the adventitial ISF. Correspondingly, the effects of the respiratory rate, tidal volume, and the I/E ratio were consistent with those under physiological conditions (Figs. 2e, 2e1, 2g, 2g1, 2i, 2i1).

To-and-fro motion of adventitial ISF along femoral vein during a cardiac and respiratory cycle

When the heartbeat and the breathing of the freshly deceased rats stopped, we used the cardiac compression or mechanical ventilation to simulate a cardiac and respiratory cycle. The same methods were used to detect the motions of the longitudinal adventitial ISF flow along the femoral veins. Under the actions of repeated chest compressions at intervals of 2-3sec, the contraction and dilation of the heart can also cause the same pulsatile flow of the adventitial ISF (Fig. 3a). In physiological state, the contraction and dilation of the atria and ventricles are not synchronized but occur one after the other. Therefore, we opened the chest cavity to directly compress the atria or ventricles at an interval of 10-15sec. It was found that every compression of the atria (Figs. 3b, 3b1) or ventricles (Figs. 3c, 3c1) induced a centrifugal motion of the adventitial ISF, and every dilation of the atria (Figs.

3b, 3b2) or ventricles (Figs. 3c, 3c2) caused a centripetal motion. In one respiratory cycle, the expansion of the lungs during inspiration caused the adventitial ISF to move centrifugally (Figs. 3d, 3d1), while the contraction of the lungs during expiration caused a centripetal movement of the adventitial ISF (Figs. 3d, 3d2).

To identify the effects of blood flow fluctuations on the adventitial ISF flow in the PACT pathways, we constructed an animal model in which the repeated cardiac compressions did not induce blood flow by opening the apex of the heart and exposing to air (Fig. S4c). Meanwhile, the adventitia of the right femoral vessels was disrupted by collagenase I, and the left femoral vessels were bathed in NS. After the administration of FluoNa into the PACT pathways of the left and right saphenous vessels, the heart was pressed at the interval of around 2sec, and the mechanical fluctuations of the left and right femoral vessel walls were measured by a laser vibrometer (OFV-5000, Polytec). It was found that the FluoNa in left lower leg was "pulled" centripetally and stained the left femoral vessel walls (Figs. S4e, S4e1). Although the mechanical fluctuations were detected on the right femoral vessels, the FluoNa only diffused locally and did not flow centripetally (Figs. S4b, S4b1). These results were consistent with our previous findings, [12-15] indicating that the flow of adventitial ISF was not dominated by blood flow and mechanical fluctuations of the vessel walls that were generated by the heartbeats (Figs. S4a, S4d).

To further determine the effects of the respiratory cycle on adventitial fluid flow, we clamped the root of the main pulmonary artery and the thoracic segment of the inferior vena cava with vascular clamps. When the root of the main pulmonary artery was clamped, the expansion and contraction of the lung can still cause the to-and-fro motions of the adventitial ISF along the femoral vein. However, after clipping of the thoracic segment of the inferior vena cava, the movements of the adventitial ISF along the femoral vein disappeared. These results suggested that effects of the lungs' expansions and contractions on the adventitial ISF flow along the systemic venous vessels were achieved through the pulmonary venous vessels, rather than the pulmonary arteries.

Qualitative observations on the circulatory cycle of adventitial ISF along the systemic and pulmonary vasculature

To depict the circulatory cycle of adventitial ISF along the systemic vasculature, we tracked the adventitial ISF flow in the PACT pathways with several major systemic arteries and veins. Firstly, after the adventitial infusion of the FluoNa into the PACT pathways of the saphenous vessels, the FluoNa from the lower limb was found to stain the PACTs of inferior vena cava (Figs.S5e-g), aorta

(Figs. S5b-d), and the heart muscles of the left ventricle (Fig. 4b). Additionally, the FluoNa infused into the PACT pathways of the axillary artery and vein (Figs.S5k-m), and the carotid artery (Figs.S5h-j) was found to stain the right anterior vena cava (Figs. S5n-p), aorta, and the heart. These data suggested that the adventitial ISF flow in the PACT pathways centripetally along both arteries and veins of the systemic vasculature into the heart, which is not the results of blood circulation.

To determine whereabouts the adventitial ISF entered the heart, we investigated the cardiac perfusion by adventitial infusion and intravenous injection of the FluoNa or silver nitrate, respectively. At 3 minutes after the adventitial infusion of the FluoNa into the PACT pathways of the lower limb, the fluorescence intensity in the myocardium (Fig. 4b) was stronger than that of hemoperfusion by intravenous injection (Figs.4c, 4d). The SMCT also showed that the silver nitrate from the PACT pathways of saphenous vessels have entered the ventricular muscles (Fig. 4e, Video 5), the amount of which was much more than those by hemoperfusion (Fig. 4f).

To delineate the cycle of adventitial ISF flow along the pulmonary vasculature, we studied the chronological distributions of FluoNa along the pulmonary vessels at the level of the right middle lobe of lungs. At 50sec after the adventitial infusion, the FluoNa from the PACT pathways of the saphenous vessels have stained the PACT pathway of the pulmonary artery but not stained the PACT pathways of the vein and the perivascular tissues (Figs. 4h, 4k). This is significantly different from the results of hemoperfusion at 50sec after the intravascular FluoNa (Figs. S6a-c). Then, at 2min, the PACT pathways of both the pulmonary artery and vein were stained (Figs. 4i, 4k); at 3min, the PACT pathways of the pulmonary artery and vein as well as the perivascular tissues in between have been stained together (Figs. 4j, 4k). The findings indicated that the adventitial ISF flow cycle along the pulmonary vasculature is from the heart into the lungs via the pulmonary arteries and back to the heart via the pulmonary veins.

Regarding the beating heart, when the FluoNa was infused into the superficial tissues on the ventricular apex, the FluoNa was found to flow in the PACT pathways along the coronary arteries toward the base of the heart (Figs. S7a-c, Video 6), suggesting that the upper part of the heart above the coronary sulcus might be the driver for the adventitial ISF flow along the coronary arteries of the ventricles.

We also explored the adventitial ISF circulatory pathways for drug delivery. By comparison of adventitial infusion with intravenous injection of Esmolol in rats, the effects on HR reduction in adventitial infusion group was slower than that in intravenous injection group at 1-3min after the

administration (Fig. S8a). The changes of Esmolol concentration detected in the myocardium of the ventricular apex coincided with the changes of the HR reduction by either adventitial infusion or intravenous injection (Fig. S8b). The Esmolol concentration of intravenous injection increased rapidly and reached the peak at 1min. The Esmolol concentration of adventitial infusion increased slowly and reached the peak at 3min.

Discussion

Building on previous findings on a long distant ISF flow pathway in animals and humans [12-15], we have identified an adventitial ISF circulatory pathway and its two regulators -- the heart and lungs. Under physiological conditions of rats, the heart and lungs work together to regulate the adventitial ISF to flow centripetally along the major arteries and veins of the systemic vasculature to the epicardium and myocardium, then into the lungs via the pulmonary arteries and return to the heart via the pulmonary veins, forming an adventitial ISF circulatory cycle. In the processes of the ISF circulating in the long-distant PACT pathways, it was found that the FluoNa reaching the lower limbs, heart or lungs had entered the blood circulation in about 10 seconds after the administration (Table S5). Accordingly, the locations where the ISF enters and leaves blood circulation should be the capillaries and follow the Starling principle of fluid exchange [26]. Unlike the blood circulation transports plasma inside the vascular circuits and can only exchange fluid with the interstitial spaces when it reaches the capillaries, an adventitial ISF circulation is not a closed loop but an open circulatory cycle in which the ISF flows along the systemic and pulmonary vasculature, and diffuses into the intercellular spaces between the tissue cells along the way. We propose that the heart and lungs can regulate the adventitial ISF to circulate along the arteries and veins as well as the arterioles, venules and capillaries in diverse tissues or organs, comprising an adventitial ISF circulatory system for fluid transport or drug delivery.

The dynamic patterns of the heart and lungs to regulate the adventitial ISF circulation are unique. Every stroke of the cardiac diastole and systole with each heartbeat, or the expansion and contraction of the lungs with each breath will generate a driving force to pull the adventitial ISF toward the heart or push the adventitial ISF away from the heart (Fig. 3). Using the STV, we were able to reveal a synergistic effect of each contraction and enlargement of the heart or lungs on adventitial ISF flow along the femoral veins by measuring the to-and-fro motions of fluorescent speckles. In dead rats, the adventitial ISF along the femoral vein was pulled toward the heart when the atria or ventricles dilated,

or the lungs contracted, whereas the adventitial ISF was pushed away from the heart when the atria or the ventricles contracted, or the lungs expanded (Fig. 3). In living rats, the compounded actions of regular heartbeats and irregular breathing generated a pulsatile and constant flow of adventitial ISF along the veins of the systemic vasculature into the myocardial tissues. Due to the lack of quantitative observation methods of fluid flow in an arterial PACT pathway, future studies are needed on the effects of each stroke of the heart and lungs on the adventitial ISF flow along the systemic arteries as well as the pulmonary arteries and veins.

The mechanisms that every cyclic deformation of either the heart or lungs can generate a pair of to-and-fro driving forces to pull or push an adventitial ISF toward or away from the heart are unknown. Unlike the heart pumping blood inside the atrial and ventricular chambers, our data showed that both the heart and the lungs can drive an adventitial ISF to flow along the vasculature as well [14,15]. Thus, we propose a working hypothesis for the mechanisms driving adventitial ISF flow: 1, When the heart and lungs expand and contract, the interstitial connective tissues within the heart and lungs work as a driver under cyclic deformations, named as "matrix or gel pump". 2, The mechanisms by which the matrix pumps can generate forces may be related to the pressure gradients caused by the deformations of the matrix, or the fluctuations of the interfacial interactions inside the cardiac and pulmonary matrix, respectively. 3, The adventitial ISF flow along the vascular vessels is the result of the synergy of three pairs of to-and-fro forces generated by the atrial, ventricular, and pulmonary matrix pumps. Under physiological conditions, it was usually observed that the adventitial ISF flowed centripetally along the systemic vasculature. In the rats with very low HR, the adventitial ISF was found to flow centrifugally along the femoral vein (Video 7). As future works, the synergistic effects of heartbeat and respiration under different conditions on the flow of adventitial ISF require more explorations.

Different from blood transport in a sealed endothelial conduit, we have revealed that the ISF flow along the blood vessels comprises two patterns, a longitudinal flow along the vessels, and diffusion to the perivascular connective tissues along the way [12,15]. When the perivascular tissues were stripped, it was found that the involved structures for the longitudinal adventitial ISF flow were the tunica adventitia surrounding by layers of fascia (Figs. 1c, 1d, S2, S3). In a linear channel within the femoral venous adventitia, the distributions of the ISF velocity were basically consistent (Figs. 1h-k), rather than a parabolic distribution in the perivascular spaces (PVS) of brain [25]. These results suggest that there is a more complex spatial structure for the longitudinal ISF flow in the adventitial channels, and its relationship with the PVS needs further studies. Here, we speculate that the outermost layer of a

vascular vessel includes at least two topologically connected spaces for fluid flow along the vasculature. One is between the adventitia and its surrounding layers of fascia, and the other is between the adventitia and tunica media. When fluid enters such interspaces of adventitial matrix, the ISF will flow along the vessels driven by the repeated heartbeats and respiration. By the conventional angiography, we found that the fluorescent ISF have stained the adventitial channels and the arterial walls of the femoral vessels after the FluoNa was injected intravenously (Video 8), indicating that the ISF derived from the capillaries would enter a PACT pathway of the lower limb in addition to being reabsorbed by venous vessels under physiological conditions. In experiments where opening the apex to interrupt blood flow, the FluoNa can flow centripetally through the intact femoral PACT pathways driven by the repeated compressions on the heart, which may be due to the fluctuations or oscillations of the vessel walls (Fig. S4) [25,27]. Whereas, even if the mechanical fluctuations of the femoral vessel walls were detected, the FluoNa could not flow along the vessel walls where were disrupted by type I collagenase, suggesting that blood flow or fluctuations of the vessel walls were not the primary causes of adventitial ISF flow.

In addition to the transport of fluid and dissolved constituents, the adventitial ISF circulatory pathways are also capable of delivering a drug. The time to peak concentration of Esmolol in the ventricular myocardium was 3 minutes for adventitial Esmolol, which was slower than 1 minute for intravenous Esmolol (Fig. S8b). The effects on the HR reduction of Esmolol by adventitial infusion was a slow pattern compared to the rapid reduction by the intravenous injection (Fig. S8a). Prospectively, an adventitial ISF circulatory pathway might be a promising organ-targeted extravascular drug delivery route.

In summary, our studies revealed that each dilation and contraction of the atria, ventricles, or lungs can generate a to-and-fro motion of the adventitial ISF along the systemic and pulmonary vasculature, and work synergistically to drive the ISF throughout the body under physiological conditions. In addition to the local diffusion and reabsorption into capillaries, fluid in the interstitium can be directly regulated by the heart and lungs and redistributed and spread by an adventitial ISF circulatory system. Subsequent studies on the detailed kinematics of the adventitial ISF circulatory pathways and the dynamics of matrix pumps will likely contribute to ascertain diverse long-range ISF flow in other anatomical sites. Further studies on the potential drug metabolism characteristics in adventitial ISF circulatory pathways may facilitate a novel therapeutic strategy for drug delivery. Future investigations on the physiological and pathophysiological functions of the adventitial ISF

circulation will comprehend the vascular, heart and pulmonary diseases, especially in the human body.

Methods and materials

Subjects

All experiments were approved by the animal ethics committee of Chinese Academy of Medical Sciences (No. ACUC-A02-2021-017) and an effort was made to minimize the number of animals used. Male Sprague-Dawley rat, 300-350 g of weight (HFK Bio-Technology, Beijing), were anesthetized with sodium pentobarbital (50 mg/kg, intraperitoneally). The ventilator (V-100, YUYAN, Shanghai, China) was used to regulate the breath, including the frequency, tidal volume, and I/E (inhalation/exhalation).

Method for adventitial infusion and intravenous injection

The skin was opened to expose the adventitia of the vessels and its surrounding layers of fascia. For adventitial infusion, a few microliters of the tracer FlouNa (4 μL, 0.1 g/L in normal saline (NS)) were dripped onto the PACT pathways on the arteries or veins of the lower, upper limbs or carotid artery using a pipette. This approach maximized access to the PACT pathways for most tracers, rather than the perivascular tissues. The total dosage of FlouNa (40 μL, 0.01 g/L in NS) used for intravenous injection was intentionally kept the same as those by adventitial injection.

After the infusion of the FluoNa into the PACT pathways of lower limbs, epicardium, and perivascular tissue in the middle lobe of the right lung, the time for fluorescein to enter the blood circulation was calculated by observing the increase of fluorescence intensity in urine. Each site contained 5 rats.

Image acquisition by fluorescence stereomicroscope or microscope

The fluorescent adventitial ISF flow in a PACT pathway along the vessels, the heart, or lungs was recorded by the fluorescence stereomicroscope (Axio Zoom.V16, Zeiss). The real-time flow of the FluoNa was acquired by a high-sensitivity camera (Prime BSI Scientific CMOS, Teledyne). The frozen cross-sectional samples were examined by the fluorescence microscope (Scope.A1, Zeiss, German) with a digital camera (Axiocam 506, Zeiss). Either controlled samples by the adventitial infusion of NS or the fluorescently stained samples were recorded by the same parameters, including the exposure time, magnification, and luminous intensity under a dark environment. The mechanical fluctuations of the left and right femoral vessel walls were measured by a laser vibrometer (OFV-5000, Polytec).

Histological analysis of the sampled PACT pathways and tissues

Each control and experimental group contained 3 rats. In the fluorescent frozen-sectional images, according to the length of the arterial or venous vessel wall, it was divided into 5 equal parts, and the fluorescence intensity in the brightest area of fluorescence in each part was recorded respectively, including the adventitia of the arteries, the adventitia of the veins, and the perivascular tissue. In the slice of myocardial tissue, the myocardial tissues around the blood vessel were chosen, and 5 areas were selected on average around the blood vessel, and the data of the fluorescence intensity were recorded. Thus, each group included a total of 15 fluorescence intensities. Fluorescence intensity analysis was performed by the ZEN 3.2. All frozen slices were studied by Elastica van Gieson staining. The hematoxylin and eosin (H&E) staining and the immunostaining of the antibodies against CD31 (Servicebio, Wuhan, China) were performed according to routine procedures.

Detection of the distributions of silver nitrate in tissues by spectral micro-computed tomography (SMCT)

The silver nitrate solution (4μL, 20% in deionized water) was infused into the PACT pathways of the saphenous vessels. The intravenous silver nitrate (40μL, 2% in deionized water) was injected into the saphenous vein slowly. If the rats died during the injection, the repeated chest compressions (400 bpm) were given immediately to ensure the circulate of the silver nitrate in the blood to reach 3 minutes. The rats were sacrificed at 3min after the administration. The samples of the downstream femoral artery and vein (2cm from the infusion site), the heart and lungs were sampled. All samples were treated with alcohol gradient dehydration (30%, 50%, 75%, 90%, 100%) before SMCT scanning. The samples were imaged using a photon counting detector (PCD) based spectral micro-CT scanner (The Institute of High Energy Physics, Chinese Academy of Sciences, China). The PCD (XCounter, Sweden) uses a CdTe crystal with a thickness of 0.75 mm as the sensor material. The detector contains 2,048×512 pixels with a pixel size of 100 μm. It has two energy thresholds and can detect photons with energy range from 10 keV to 160 keV. By setting the thresholds, two energy window data can be obtained in one CT scan. [17-19].

Fluorescent speckle tracking velocimetry

Speckle pattern translation recording has been extensively used in measuring in-plane displacements [20,22,23]. By analyzing the data of the fluorescent adventitial ISF flow, we developed a method of Speckle tracking velocimetry (STV) to measure the to-and-fro motions of fluorescence along the vessels. 4 steps were included: 1) High-pass filter; 2) Image registration; 3) Mean-image subtraction; and 4) Velocimetry. After the first 3 steps, the input image sequence was transformed into

an image sequence purely including speckle motion. A region of interest (ROI) was then manually delineated, which included the speckle motions along the vessels. The ROI area was then divided into small patches. Afterwards, cross-correlation [21] was performed to estimate the most probable displacement within each surrounding area. Displacement per time between adjacent images yielded the velocity. The speed change curves were matched to the changes of heartbeats and respiration acquired by animal physiological monitoring device (RM6240, YUYAN, Shanghai, China).

The compression of the atria and ventricle

After the chest cavity was opened, the compressions of the atria or ventricle were performed by a digital force gauge (HF-10, HighTec, Suzhou, China) at the force around 0.5 N. The frequency, duration of one-shot or continuous compressions were adjusted according to the experiments.

Esmolol administration and concentration in myocardium analysis

The changes of the heart rate by adventitial infusion or intravenous injection of Esmolol was recorded in 10 alive rats, respectively. The dosage of Esmolol for adventitial infusion or intravenous injection was 0.5 mg/kg and adjusted according to each rat weight [28]. After the adventitial infusion or intravenous injection of Esmolol, another 50 rats were sacrificed at 1, 3, 5, 8, 35min, respectively. The concentration of Esmolol in ventricular muscles was detected by LC-MS/MS. The samples were at homogenized with 1 μL/mg of methanol acetonitrile (50:50) % (v/v), centrifuged at 4000 rpm (Eppendorf 5810R) for 20 minutes, and the supernatant was taken for detection. Measurements of the Esmolol were accomplished on a Shimadzu LC-2-AD XR equipped with a binary pump, a degasser, an auto sampler/injector and a column heater (Shimadzu, Kyoto, Japan), coupled to an AB SCIEX QTrap 5500 Mass Spectrometer equipped with an ESI ionization source (AB SCIEX, Los Angeles, CA, USA).

Statistical analysis

Significant comparisons of all statistical data were performed by *t*-test. All testing was two-tailed and exact P values were calculated at a 0.05 level of significance and stated in the figure legends.

Author contributions

HY.L. conceived the original ideas and concepts. HY.L., H.L., C.M., and FS.J. designed the experiments. HY.L. wrote the paper. B.L., W.Qi.L., X.Q., HY.L., JZ.L., Z.H., XX.W., X.Y., DH.H. performed the experiments. Y.H., B.L., H.L. calculated the velocity. CZ.Y., ZM.L., and T.G. prepared the spectral micro-CT. HY.L., C.M., FS.J., J.H., and ZJ.Z. analyzed the imaging data. W.Qing.L., F.W., and XX.L. analyzed the data for drug delivery experiments.

HY.L. and B.L. prepared pictures and videos.

Acknowledgements

We thank Professors Guanhua Xu, Yixin Zeng and Kaixian Chen, Weiwu Hu, Saicang Lobsang Hwardan Chegynima, Jamyang Danchour and Angwen zhabar for their fruitful discussions. We thank Weihua Wang, Fang Wei, Yu Tang in center of pharmaceutical technology of Tsinghua University for their help in LC-MS/MS.

Funding

This work was supported by National Natural Science Foundation of China (82050004), Innovation Team and Talents Cultivation Program of National Administration of Traditional Chinese Medicine. (No: ZYYCXTD-D-202202), and Beijing Hospital Clinical Research 121 Project (121 - 2016002).

Conflict of interest statement

None declared.

References

1 Aird, W. C. Discovery of the cardiovascular system: from Galen to William Harvey. *Journal of Thrombosis and Haemostasis* **9**, 118-129 (2011). https://doi.org:10.1111/j.1538-7836.2011.04312.x

2 Elshahed, M. Blood flow in capillary under starling hypothesis. *Applied mathematics and computation* **149**, 431-439 (2004). https://doi.org:10.1016/S0096-3003(03)00151-6

3 Levick, J. R. Flow through interstitium and other fibrous matrices. *Q J Exp Physiol* **72**, 409-437 (1987). https://doi.org:10.1113/expphysiol.1987.sp003085

4 Hall JE, G. A. *The microcirculation and lymphatic system. In: Guyton and Hall Textbook of Medical Physiology, 12th Ed.* 180-182 (Philadelphia, 2011).

5 Casley-Smith, J. R. Calculations relating to the passage of fluid and protein out of arterial-limb fenestrae, through basement membranes and connective tissue channels, and into venous-limb fenestrae and lymphatics. *Microvasc Res* **12**, 13-34 (1976). https://doi.org:10.1016/0026-2862(76)90003-0

6 Hauck, G. The connective tissue space in view of the lymphology. *Experientia* **38**, 1121-1122 (1982). https://doi.org:10.1007/bf01955400

7 Woollam, D. H. & Millen, J. W. The perivascular spaces of the mammalian central nervous system and their relation to the perineuronal and subarachnoid spaces. *J Anat* **89**, 193-200 (1955).

8 Iliff, J. J. *et al.* A paravascular pathway facilitates CSF flow through the brain parenchyma and the clearance of interstitial solutes, including amyloid beta. *Sci Transl Med* **4**, 147ra111 (2012). https://doi.org:10.1126/scitranslmed.3003748

9 Wardlaw, J. M. *et al.* Perivascular spaces in the brain: anatomy, physiology and pathology. *Nat Rev Neurol* **16**, 137-153 (2020). https://doi.org:10.1038/s41582-020-0312-z

10 Butler, T. P., Grantham, F. H. & Gullino, P. M. Bulk transfer of fluid in the interstitial compartment of mammary tumors. *Cancer Res* **35**, 3084-3088 (1975).

11 Pathak, A. P. *et al.* Characterizing extravascular fluid transport of macromolecules in the tumor interstitium by

magnetic resonance imaging. *Cancer Res* **65**, 1425-1432 (2005). https://doi.org:10.1158/0008-5472.Can-04-3682

12 Li, H. Y. *et al.* Fluid flow along venous adventitia in rabbits: is it a potential drainage system complementary to vascular circulations? *PLoS One* **7**, e41395 (2012). https://doi.org:10.1371/journal.pone.0041395

13 Li, H. Y. *et al.* A long-distance fluid transport pathway within fibrous connective tissues in patients with ankle edema. *Clin Hemorheol Microcirc* **63**, 411-421 (2016). https://doi.org:10.3233/ch-162057

14 Li, H. Y. *et al.* An extravascular fluid transport system based on structural framework of fibrous connective tissues in human body. *Cell Prolif* **52**, e12667 (2019). https://doi.org:10.1111/cpr.12667

15 Li, H. Y. *et al.* Layers of interstitial fluid flow along a "slit-shaped" vascular adventitia. *J Zhejiang Univ Sci B* **22**, 647-663 (2021). https://doi.org:10.1631/jzus.B2000590

16 Li, H. Y. *et al.* Active interfacial dynamic transport of fluid in a network of fibrous connective tissues throughout the whole body. *Cell Proliferation* **53**, e12760 (2020). https://doi.org:10.1111/cpr.12760

17 Badea, C. T. *et al.* Dual-energy micro-CT of the rodent lung. *American Journal of Physiology-Lung Cellular and Molecular Physiology* **302**, L1088-L1097 (2012). https://doi.org:10.1152/ajplung.00359.2011

18 Li, M. *et al.* A study on noise reduction for dual-energy CT material decomposition with autoencoder. *Radiation Detection Technology and Methods* **3** (2019). https://doi.org:10.1007/s41605-019-0122-2

19 Zhang, Z. *et al.* An Optimized K-Edge Signal Extraction Method for K-Edge Decomposition Imaging Using a Photon Counting Detector. *Frontiers in Physics* **8** (2021). https://doi.org:10.3389/fphy.2020.601623

20 Adrian, R. J. Scattering particle characteristics and their effect on pulsed laser measurements of fluid flow: speckle velocimetry vs particle image velocimetry. *Appl Opt* **23**, 1690-1691 (1984). https://doi.org:10.1364/ao.23.001690

21 Keane, R. D. & Adrian, R. J. Theory of cross-correlation analysis of PIV images. *Applied scientific research* **49**, 191-215 (1992). https://doi.org:10.1007/BF00384623

22 Raffel, M., Willert, C. E. & Kompenhans, J. *Particle image velocimetry: a practical guide*. Vol. 2 (Springer, 1998).

23 Thielicke, W. & Sonntag, R. Particle Image Velocimetry for MATLAB: Accuracy and enhanced algorithms in PIVlab. *Journal of Open Research Software* **9** (2021). https://doi.org:10.5334/jors.334

24 Hadaczek, P. *et al.* The "perivascular pump" driven by arterial pulsation is a powerful mechanism for the distribution of therapeutic molecules within the brain. *Mol Ther* **14**, 69-78 (2006). https://doi.org:10.1016/j.ymthe.2006.02.018

25 Mestre, H. *et al.* Flow of cerebrospinal fluid is driven by arterial pulsations and is reduced in hypertension. *Nat Commun* **9**, 4878 (2018). https://doi.org:10.1038/s41467-018-07318-3

26 Levick, J. R. & Michel, C. C. Microvascular fluid exchange and the revised Starling principle. *Cardiovasc Res* **87**, 198-210 (2010). https://doi.org:10.1093/cvr/cvq062

27 Kedarasetti, R. T., Drew, P. J. & Costanzo, F. Arterial pulsations drive oscillatory flow of CSF but not directional pumping. *Sci Rep* **10**, 10102 (2020). https://doi.org:10.1038/s41598-020-66887-w

28 Sasao, J. *et al.* In rabbits, landiolol, a new ultra-short-acting β-blocker, exerts a more potent negative chronotropic effect and less effect on blood pressure than esmolol. *Canadian journal of anaesthesia* **48**, 985-989 (2001). https://doi.org:10.1007/BF03016588

Figures and legends

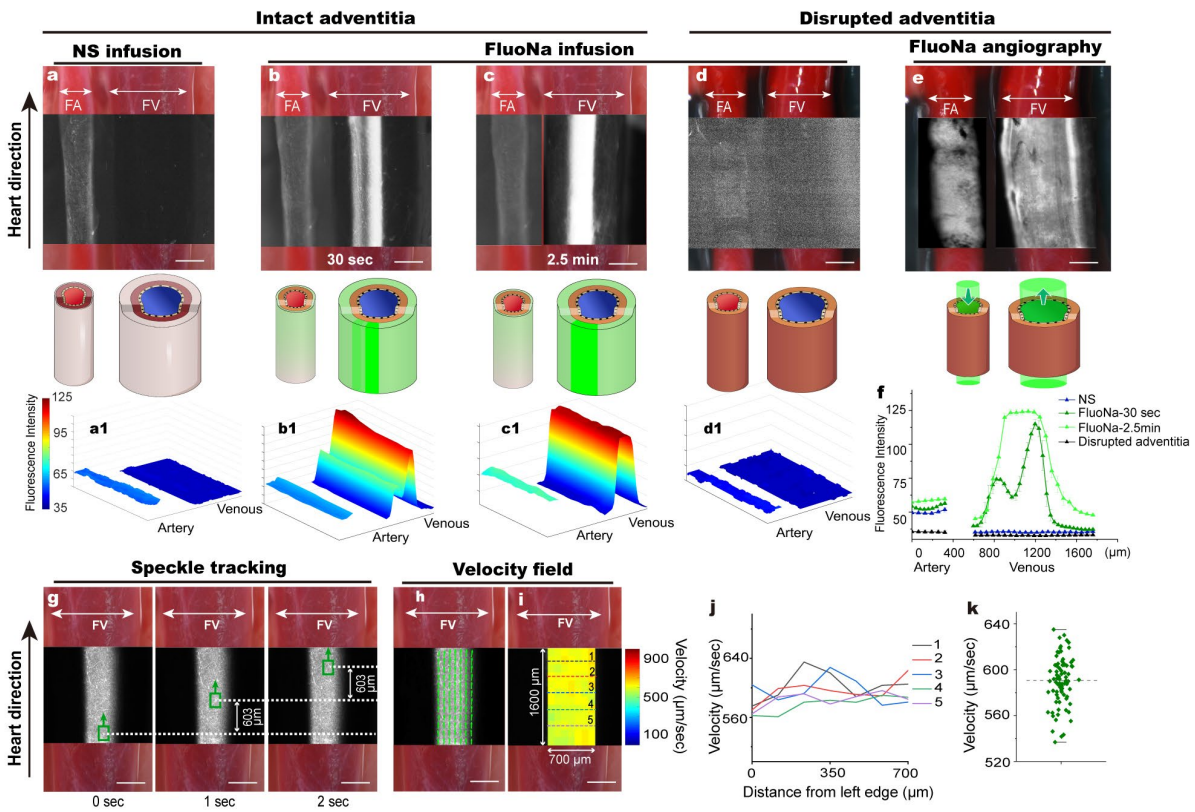

Figure 1. Quantifying the longitudinal adventitial ISF flow along the femoral artery and vein that were stripped of perivascular tissues.

To clearly observe the longitudinal adventitial ISF flow, the femoral arteries and veins (**a**, **b**, **c**, **d**, **e**) were stripped of the perivascular connective tissues. By fluorescence stereomicroscope, a, a1 showed that the fluorescence intensity of a femoral artery and vein was weaker by the adventitial infusion of NS. After the adventitial infusion of FluoNa into the upstream PACT of the saphenous vessels, two linear fluorescent adventitial channels were found along one side of the femoral vein at 30sec (**b**) and converged into one linear channel at 2.5min (**c**). When the adventitia of femoral vessels was disrupted by collagenase I (**d**), the upstream FluoNa cannot flow through and stain the adventitial walls of the artery and vein. Meanwhile, the contralateral venous angiography confirmed that this femoral artery (**d**) was unobstructed, and the ipsilateral venous angiography showed this femoral vein (d) was also unobstructed (**e**). **a1**, **b1**, **c1**, **d1** showed that the distributions of the fluorescein along the arteries and veins. **f** showed that the changes in fluorescence intensity of the (**a1**, **b1**, **c1**, **d1**). The longitudinal adventitial ISF flow along the femoral vein exhibited speckle-like motions of FluoNa (**g**) and speckle tracking velocimetry was performed accordingly. **h** The velocity field (green arrows) showed that

adventitial ISF flow was in the same direction as the blood flow. **i**, **j** The flow speed profiles showed that the region of the adventitial ISF flow from the left edge of the linear adventitial channel was nearly uniform but not a parabola. **k** Median flow speed was 590.2μm/sec (dotted line, 536.8μm/sec, 635.0μm/sec). The HR of the rat was 360bpm, the respiratory rate was 90, I/E was 1:1.6, and tidal volume was 4.5mL. Scale bar: 500 μm. **FA**, femoral artery. **FV**, femoral vein.

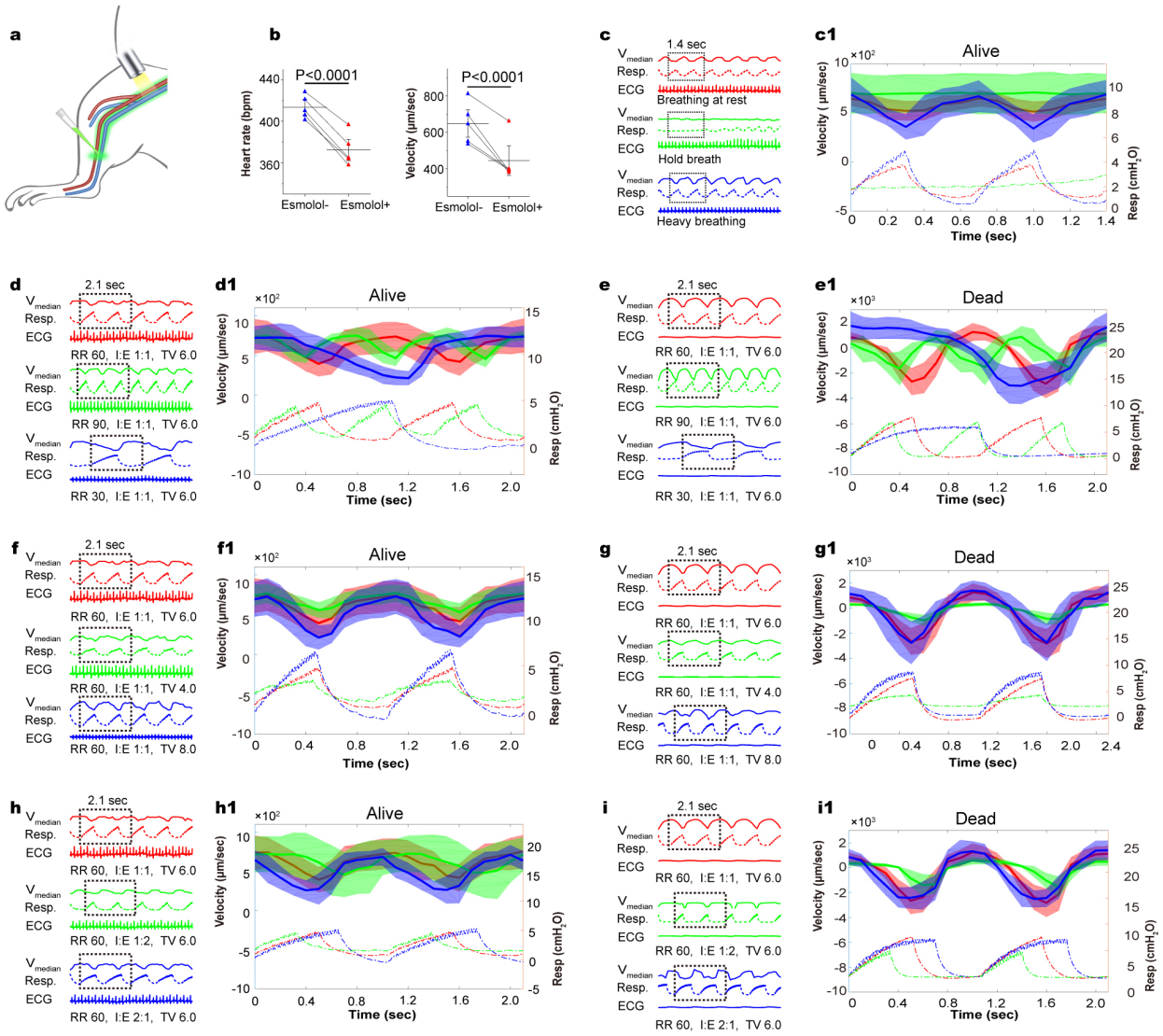

Figure 2. Regulation of adventitial ISF flow in the femoral PACT pathways by HR and respiration.

a Illustration of the observation on the adventitial ISF flow in the PACT pathways of the femoral vessels. **b** When the HR reduced by the intravenous Esmolol, the speed of adventitial ISF flow

decreased. (*t*-test, mean ± SEM, n = 5) **c**, **c1** When the breath held, like apnea, the adventitial ISF flow rate increased by comparison with that at resting breath. A heavy breath induced a pulsatile flow at the same frequency as the heavy breath. **d**, **d1**, **e**, **e1** The frequency of the pulsed flow was consistent with the respiratory rate in alive or dead rats. **f**, **f1**, **g**, **g1** The greater the tidal volume, the greater the pulse amplitude of adventitial ISF flow in alive or dead rats. **h**, **h1**, **i**, **i1** The inspiration and expiration (I/E) ratio (1:1, 2:1, 1:2) determined the descending and ascending branches of the pulse in alive or dead rats. In alive rats, the inhalation can decelerate the centripetal adventitial ISF flow. In dead rats, the inhalation can cause a centrifugal adventitial ISF flow, while the exhalation induced a centripetal adventitial ISF flow. Each group of (**c**, **d**, **e**, **f**, **g**, **h**, **i**) was sampled from 6 rats.

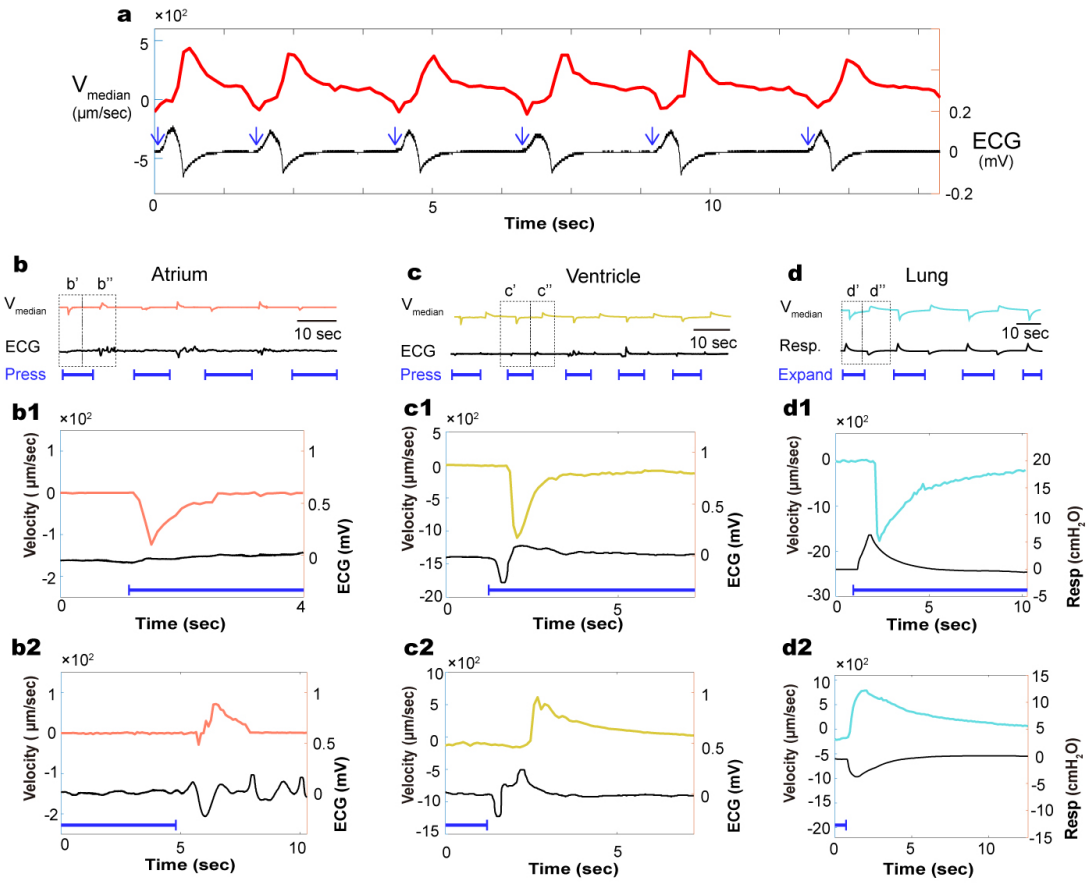

Figure 3. To-and-fro motion of adventitial ISF in the femoral PACT pathways during a cardiac and respiratory cycle

a By repeated chest compressions at intervals of 2-3sec in the freshly deceased rats, the contraction and dilation of the heart caused the same pulsatile flow of the adventitial ISF along the femoral veins. Blue arrow indicates the one-shot act of chest compression. When the chest cavity was opened, the atria or ventricles were continuously compressed for 10-15sec (blue line), and then released to allow

the atria or ventricles to dilate on their own (**b**, **c**). **b1**, **c1** The compression of the atria or ventricles induced a centrifugal adventitial ISF flow. **b2**, **c2** The dilation of the atria or ventricles caused a centripetal adventitial ISF flow. **d** The lungs were expanded by the 5ml syringe for 10-15sec (blue line), and then contracted by the 5ml syringe for another 10-15min. **d1** The expansion of the lungs induced a centrifugal adventitial ISF flow. **d2** The contraction of the lungs caused a centripetal adventitial ISF flow.

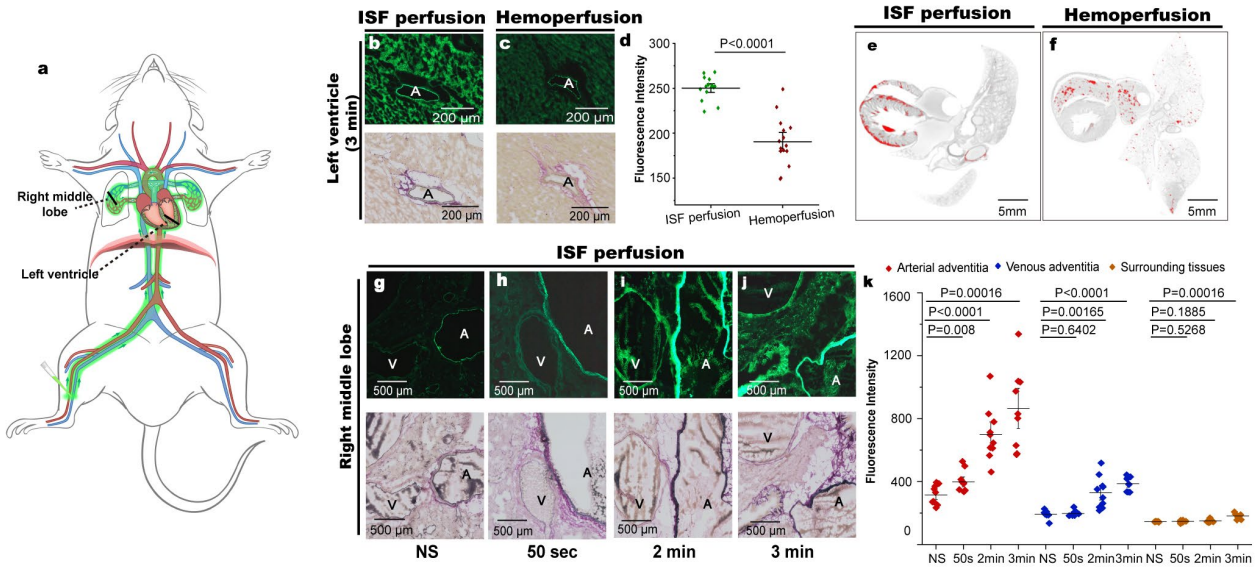

Figure 4. Qualitative observations on adventitial ISF perfusion and intravenous perfusion of the FluoNa or silver nitrate into the heart, and the circulatory cycle of adventitial ISF along the pulmonary vasculature

At 3min after the adventitial infusion of FluoNa from the PACT pathways of the lower limb or the intravenous injection of FluoNa, the fluorescence intensity (**b**) of the myocardium by adventitial infusion (**a**) was significantly stronger than those by intravenous injection (**c**). By SMCT, the silver nitrate from the PACT pathways of the lower limb was found in the left and right ventricular muscles (**e**) significantly but few in the lungs. In contrast, the silver nitrate by intravenous injection was found inside the right ventricle, some coronary arteries, and pulmonary vessels (**f**). To delineate the adventitial ISF cycle of the pulmonary vasculature, FluoNa was infused into the PACT pathways of the lower extremities and detected in the middle lobe of the right lung at different times. **g** The cross-sections showed a pulmonary artery and vein in the middle lobe and sampled at 50sec after the adventitial infusion of NS. **h** At 50sec after the adventitial infusion, the upstream FluoNa stained the PACT pathway of the pulmonary artery but not the PACT pathways of the vein and the perivascular tissues. **i** At 2min after the adventitial infusion, the upstream FluoNa stained the PACT pathway of

the pulmonary artery and vein but not the perivascular tissues. **j** At 3min after the adventitial infusion, the upstream FluoNa stained the PACT pathway of the pulmonary artery and vein and the perivascular tissues. **k** The changes of the fluorescence intensity of the PACT pathways in arteries, veins and the surrounding tissues, respectively. The findings indicated that the adventitial ISF flow cycle along the pulmonary vasculature is from the heart to the lungs along the pulmonary arteries, and from the lungs to the heart along the pulmonary veins. In (**d**, **k**), *t*-test, mean ± SEM, n = 3. **A**, artery. **V**, vein. The sites of cross section in in heart (**b**, **c**) and lung (**g**-**j**) were pointed at (**a**) as the black solid lines.